Archival Report

A Ventromedial Prefrontal-to-Lateral Entorhinal **Cortex Pathway Modulates the Gain of Behavioral Responding During Threat**

Erin Hisey, Alicia Purkey, Yudong Gao, Kazi Hossain, Scott H. Soderling, and Kerry J. Ressler

ABSTRACT

BACKGROUND: The ability to correctly associate cues and contexts with threat is critical for survival, and the inability to do so can result in threat-related disorders such as posttraumatic stress disorder. The prefrontal cortex (PFC) and hippocampus are well known to play critical roles in cued and contextual threat memory processing. However, the circuits that mediate prefrontal-hippocampal modulation of context discrimination during cued threat processing are less understood. Here, we demonstrate the role of a previously unexplored projection from the ventromedial region of PFC (vmPFC) to the lateral entorhinal cortex (LEC) in modulating the gain of behavior in response to contextual information during threat retrieval and encoding.

METHODS: We used optogenetics followed by in vivo calcium imaging in male C57/B6J mice to manipulate and monitor vmPFC-LEC activity in response to threat-associated cues in different contexts. We then investigated the inputs to, and outputs from, vmPFC-LEC cells using Rabies tracing and channelrhodopsin-assisted electrophysiology.

RESULTS: vmPFC-LEC cells flexibly and bidirectionally shaped behavior during threat expression, shaping sensitivity to contextual information to increase or decrease the gain of behavioral output in response to a threatening or neutral context, respectively.

CONCLUSIONS: Glutamatergic vmPFC-LEC cells are key players in behavioral gain control in response to contextual information during threat processing and may provide a future target for intervention in threat-based disorders.

https://doi.org/10.1016/j.biopsych.2023.01.009

The ability to form associations between contexts and cues that predict negative outcomes is critical for survival, as is the ability to respond to learned cues in a context-dependent manner. Disruptions in the ability to modulate responsiveness to previously threatening cues based on context are hallmarks of fear and anxiety-based disorders, in particular posttraumatic stress disorder, in which a key diagnostic criterion is avoidance of cues and contexts associated with prior trauma that are no longer threatening (1,2). While brain regions such as the prefrontal cortex (PFC) and hippocampus are known to be critical in threat processing and context discrimination, the roles of specific projections from these and related regions in context-dependent cued threat processing are not well understood.

The ventromedial PFC (vmPFC) comprises multiple subregions and plays a multifaceted role in threat processing and retrieval. The infralimbic region of the vmPFC (IL) has historically been considered central to extinction learning or threat inhibition, while the prelimbic region of the vmPFC (PL) has been thought of as more critical to threat expression (3-6). However, other studies have suggested that IL may instead modulate context-dependent discrimination in general (7-9) rather than the specific retention of extinguished cue-based

memories. In contrast to the PFC, the hippocampus has long been known as a key player in contextual memory formation, particularly in threat conditioning (TC), in which it forms memory engrams that encode emotionally salient contexts that can be reactivated to drive threat responding in neutral contexts (10,11). Despite these findings, the cellular and circuitspecific nature of the vmPFC-hippocampal complex's role in context modulation of cued threat processing remains unclear.

As a neural hub containing dense inputs and outputs from both the PFC and hippocampus, the lateral entorhinal cortex (LEC) is poised to integrate and transform information shared between these 2 regions. In addition to the hippocampus and PFC, the LEC also provides strong feedforward inhibitory input to the basolateral amygdala (BLA) (12), which presumably allows it to modulate BLA principal cells that encode incoming sensory stimuli, placing it at a nexus to modulate encoding and retrieval of context in threat memory regulation. Previously, the LEC has been found to encode complex associations between contexts and objects in rodents (13-16); furthermore, gamma oscillations between the LEC and dentate gyrus specifically are necessary for object recognition memory (17). The LEC is also critical for long-term memory in humans (18) and is heavily implicated in Alzheimer's disease as the cortical region affected earliest by the disease (19,20). Historically, there has been conflicting evidence over the role of the LEC in TC, in part due to variable lesion sizes that overlap with the medial entorhinal cortex or due to the use of different conditioning paradigms (21–23). In some studies, lesions of the entorhinal cortex as a whole before conditioning disrupt the context-dependent nature of threat extinction, resulting in deficits in context recall (21) and a lack of threat renewal (24), whereas other studies show no effect of entorhinal lesions on contextual TC (23). Most recently, lesions in the LEC of rats have been shown to disrupt both contextual and cued memory recall in both delay and trace TC (25).

To address these remaining questions, we examined the role of an unexplored projection from anterior vmPFC (encompassing portions of anterior IL and medial orbital [MO]) to the LEC (vmPFC-LEC cells) in threat encoding and retrieval using in vivo optogenetics and anatomical and physiological characterization of vmPFC-LEC cell inputs and outputs and in vivo calcium imaging in behaving mice. We found that vmPFC-LEC cells play a critical role in the retrieval of cued threat memory in specific contexts as well as in the ability to shape encoding of contextual threat memory, flexibly shaping the gain of behavioral responding depending on the emotional salience of the context. We also found that vmPFC-LEC cells are positioned to integrate information from a variety of cortical structures and strongly modulate downstream hippocampal activity. Surprisingly, glutamatergic vmPFC-LEC cells modulate the gain of behavior in response to contextual information, though cortical gain control is often attributed to inhibitory interneurons.

METHODS AND MATERIALS

All experiments were approved by and performed in accordance with McLean Hospital Institutional Animal Care and Use Committee guidelines. Experiments were performed in P60-120 adult male C57/B6J mice (Jackson Laboratory) that were housed in a 12-hour light/dark cycle and provided food and water ad libitum.

Viral Injections and Implants

Stereotaxic viral injections were performed in adult male mice under isofluorane anesthesia, as previously described (26). AAV (adeno-associated virus) was injected in the vmPFC (encompassing anterior IL and portions of MO) (from brain surface: Allen Mouse Brain Reference Atlas: 2.3 A/P, 0.3 L, 1.5 V; AAV2/9 EF1a double-floxed hChR2(H134R)-EYFP or AAV2/9 EF1a double-floxed EYFP for channelrhodopsin-2 [ChR2] experiments; AAV2/5 EF1a-DIO-eNpHR3.0-EYFP or AAV2/5 hSyn-DIO-EGFP for halorhodopsin [Halo] experiments; AAV2/9 hSyn-flex GCaMP6f for imaging experiments) (Table S1) and/or the LEC (-3.9 A/P, 4.3 L, 2.3 V, AAVretro hSyn Cre for all Credependent experiments) (Allen Mouse Brain Atlas) over a period of approximately 10 minutes (5–10 injections of 18–32 nL every 20 seconds) with a pressure injection system (Nanoject).

For optogenetic experiments, mice were implanted unilaterally (ChR2 experiments) or bilaterally (Halo experiments) with

a fiberoptic ferrule over the vmPFC injection sites at a 7° angle (0.25-mm diameter, 0.3 numerical aperture, RWD Life Science) (Figure S7). For Inscopix imaging experiments, a 1.2×1.2 mm square of skull over the GCaMP injection site was removed, and a lens was implanted in the same position as the vmPFC injection (Proview Lens Probe, diameter 1.0 mm, length 4.0 mm; Inscopix). A small screw was also affixed to the skull above the cerebellum to increase the stability of the implant. All implants were secured to the skull with dental cement (Metabond) followed by a thin layer of tissue adhesive (VetBond).

Optogenetic Experiments

Cued TC. Mice were placed in conditioning chambers (Med Associates) (context A, lights off, ethanol for cleaning, shock grid floor) for 15 minutes to habituate them to the chamber. The next day, mice were again placed in the conditioning chambers (context A) and underwent cued TC (3 minutes of habituation followed by five 30-second 6 kHz tones terminating in a 1-second 0.7-mA shock with variable intertone intervals over a total of 14 minutes) (FreezeFrame). The following day, mice underwent their first threat retrieval (TR1) training in either context A or a different room (context B, lights on, quatricide for cleaning, smooth black plexiglass floor). The TR protocol consisted of 3 minutes of habituation in the novel chamber followed by fifteen 30-second 6 kHz tones with a 30second intertone interval. For ChR2 experiments, mice were gently restrained and coupled to a fiberoptic cable (ThorLabs) and laser (Shanghai Lasers, 493 nm for ChR2 experiments) before being placed in the chamber. Thereafter, 30-second 20-Hz blue laser light pulses (2 mW) were paired with each tone presentation during the first TR day (FreezeFrame). The following day, mice were tested for a second TR (TR2) in the same chamber in which the previous TR session occurred (3 minutes of habituation in the chamber followed by fifteen 30second 6 kHz tones with a 30-second intertone interval). To measure a true baseline for each session, as unaffected as possible by handling stress, we used the 30-second window immediately before tone 1 (baseline [BL]).

Contextual TC. Mice were placed in conditioning chambers (context C, lights off, Clidox for cleaning, black diagonal stripes on a white background on walls, shock grid floor) for 15 minutes to habituate them to the chamber. On the context conditioning day, mice were gently restrained and coupled to a fiberoptic cable/s (ThorLabs) and laser (Shanghai Lasers, 493 nm for ChR2 experiments; RWD, 561 nm for Halo experiments) before being placed in the chamber. Mice underwent contextual TC with optogenetic stimulation (2 minutes of habituation followed by 4 1-second 0.7-mA shock with variable intershock intervals over 6 minutes; continuous 20-Hz laser pulse [2 mW for ChR2, 10 mW for Halo] for minutes 2–8). The next day, mice were placed back in context C for 5 minutes to test context recall.

All videos from behavioral sessions were recorded at 30 frames per second in FreezeFrame and hand-scored in 30-second bins by an experimenter blinded to the experimental condition.

Slice Electrophysiology

For whole-cell patch clamp recordings, 300-µm horizontal slices were prepared as previously described (27) from mice expressing ChR2 in vmPFC-LEC cells. Glass pipettes (4–7 MΩ, Sutter P-97, internal solution at ~290 mOsm/L) were used to patch cells in layers 2/3 and 5 of the LEC. Light-evoked currents were recorded at -70 mV for excitatory postsynaptic currents and 0 mV for inhibitory postsynaptic currents in the presence of 1-μM tetrodotoxin and 100-μM 4-AP to isolate monosynaptic inputs. ChR2 was activated through a 20× dipping objective using a light emitting diode light source (pE-300ultra; CoolLED) with a 2-ms pulse of 460-nm light every 10 seconds, and intensity was titrated to establish a stable response (15%–30%). Series resistance was monitored throughout all recordings, and only recordings that remained stable over the recording period (\leq 30-M Ω resistance and <20% change in resistance) were included. Data were acquired using pClamp software (https://www.moldev.com) with Multiclamp 700B amplifier (Molecular Devices), digitized at 50 kHz with Digidata 1550 (Molecular Devices), and low-pass filtered at 1 kHz. All chemicals were purchased from Sigma-Aldrich, Tocris, and Abcam. For data analysis, excitatory postsynaptic current and inhibitory postsynaptic current amplitudes were manually detected and calculated offline using Clampfit (Molecular Devices). Amplitudes were calculated from 10 averaged sweeps.

Inscopix Imaging Experiments

Calcium events were collected at 20 frames per second at 50% to 60% laser power (Inscopix nVista HD) for the duration of time within the chamber. The onset of calcium imaging was synchronized with the placement of the animal in the arena for concurrent calcium imaging and behavioral tracking (Ethovision 11.5; https://www.noldus.com/ethovision-xt). At the end of each experiment, mice were perfused, and localization of viral expression and lens placement were visually confirmed with histology. Only mice with viral expression contained within the vmPFC across 3 consecutive coronal sections and correct lens placement in the vmPFC were included in this study.

The data collected from imaging sessions were processed to extract calcium event timing (Inscopix data processing 1.3.1; https://www.inscopix.com/software-analysis-miniscope-imaging). Briefly, using the Inscopix software package mentioned above, data were spatially downsampled (2-3×) and motion corrected in reference to the first frame of the recording. Cells were identified with principal component analysis-independent component analysis and confirmed as cells by eye. The calcium traces extracted from principal component analysis-independent component analysis were then thresholded (median absolute deviation: 3; event shortest decay time: 0.20 seconds), and the timing of calcium events from individual cells was calculated.

RESULTS

Activation of vmPFC-LEC Cells With Channelrhodopsin Enhances Cued Threat Expression in Initial Training Context

We first wanted to understand how vmPFC-LEC cells participate in cued threat learning and maintenance in different

contexts, specifically if vmPFC-LEC activity is critical to threat regulation during threat expression. To accomplish this, we used temporally specific manipulation of vmPFC-LEC activity during TR. To drive expression specifically in vmPFC-LEC cells, we unilaterally injected a virally encoded Cre-dependent channelrhodopsin (ChR2) (n=11) or GFP (green fluorescent protein) (n=9) into the vmPFC and a retrogradely transported virally encoded Cre into the LEC of adult male mice (Figure 1A, C). We chose to target cell bodies in the vmPFC, given the sparse collaterals from vmPFC-LEC cells in regions other than the LEC (Figure S1), as well as the difficulty of implanting a region as lateral as the LEC.

One month after viral injection, we implanted the mice with a unilateral fiberoptic cannula over the vmPFC to stimulate vmPFC-LEC cell bodies (Figure 1B). We used 5 tonefootshock pairings to threat condition the implanted mice in context A. The following day, we examined TR1 in context A with a 15-tone subthreshold extinction protocol, pairing each 30-second tone with a 30-second 20 Hz pulse of blue light. The next day, we again examined TR2 by playing back fifteen 30-second tones again in context A (Figure 1D). Though GFP and ChR2 groups showed no differences in freezing levels throughout TC (Figure 1E) (two-way repeated-measures analysis of variance [ANOVA] across 5 tones, main effect of virus condition: p = .515), ChR2 mice demonstrated increased freezing during the first 5 tone presentations of TR1 (Figure 1F) (threat expression, two-tailed unpaired t test for difference between average percent freezing across tones 1–5, p = .018). Subsequently, the next day, during TR2, ChR2 mice also showed lasting increases in tone-evoked freezing compared with control GFP mice (two-way repeated-measures ANOVA across all 15 tones, main effect of virus condition: p = .002), despite no longer being activated (Figure 1G). This increase in threat expression was not due to increases in general anxietylike behaviors: stimulation of vmPFC-LEC cells during open field testing (Figure S2A-C) and elevated plus maze (Figure S2D-F); two different assays of anxiety-like behavior that were performed before TC revealed no differences in either time in center or in open arms or distance traveled between the GFP and ChR2 groups. Given the increase in threat expression coupled with the lack of effect on anxiety-like behavior, we hypothesized that vmPFC-LEC activation might increase the gain of incoming contextual information to increase behavioral sensitivity to the current context.

Activation of vmPFC-LEC Cells Inhibits Cued Threat Expression in a Neutral Context

We next performed an identical experiment to the one described above with another cohort of mice, but now changed the context in which threat memory was retrieved (i.e., threat condition in context A, TR1 in context B+ChR2 stimulation, TR2 in B) (Figure 2A, B). Though there was no difference in freezing levels during TC in GFP and ChR2 mice (Figure 2C) (two-way repeated-measures ANOVA across 5 tones, main effect of virus condition: p = .854), ChR2 mice showed significantly decreased freezing across all 15 tones as compared with control mice (Figure 2D) (two-way repeated-measures ANOVA across all 15 tones, main effect of virus condition: p = .042) with a significant decrease in freezing

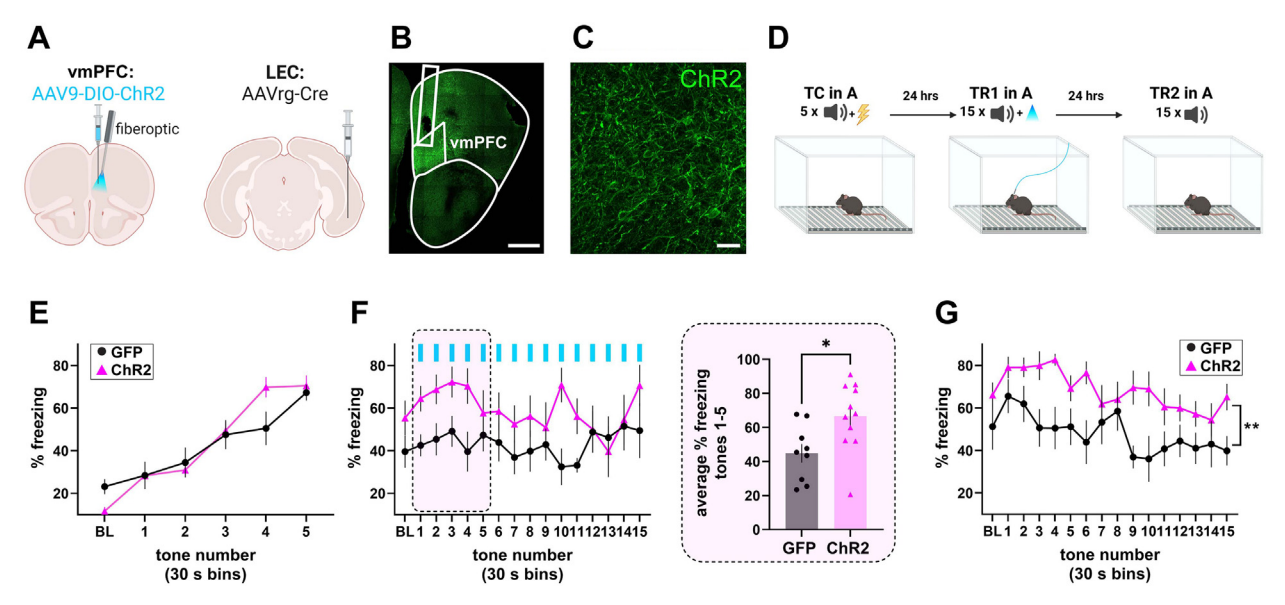


Figure 1. vmPFC-LEC cell activation in the same context as conditioning increases threat expression. (A) Schematic of viral injections and fiberoptic placement. (B) Image showing fiberoptic placement in the vmPFC and ChR2 expression throughout the vmPFC. Scale bar = 1 mm. (C) Magnified image of ChR2 expression of vmPFC-LEC cells and fibers in the vmPFC. Scale bar = 50 μ m. (D) Schematic for A-A-A TC, TR1 and TR2 paradigm. (E) Percent freezing during 30-second bins of baseline and tone presentation during TC in context A in GFP (black, n = 9) and ChR2 (pink, n = 11) animals. (F) Percent freezing during 30-second bins of baseline and tone presentation during TR1 in context A. Thirty-second 20-Hz ChR2 pulses were delivered at the onset of each 30 seconds tone. Shaded box compares average percent freezing during the first 5 tones between GFP- and ChR2-injected animals. (G) Percent freezing during 30-second bins of baseline and tone presentation during TR2 in context A. * p \leq .05, * p \leq .01. ChR2, channelrhodopsin-2; GFP, green fluorescent protein; LEC, lateral entorhinal cortex; TC, threat conditioning; TR1, first threat retrieval; TR2, second TR; vmPFC, ventromedial prefrontal cortex.

during the threat expression window (two-tailed unpaired t test for difference between average percent freezing across tones 1–5, p=.030). Though stimulation decreased freezing during threat expression in ChR2 mice, freezing levels during TR2 did

not differ between ChR2 and control mice (Figure 2E) (two-way repeated-measures ANOVA across all 15 tones, main effect of virus condition: p=.209). In light of the results presented in Figure 1, these results suggest that vmPFC-LEC cells can

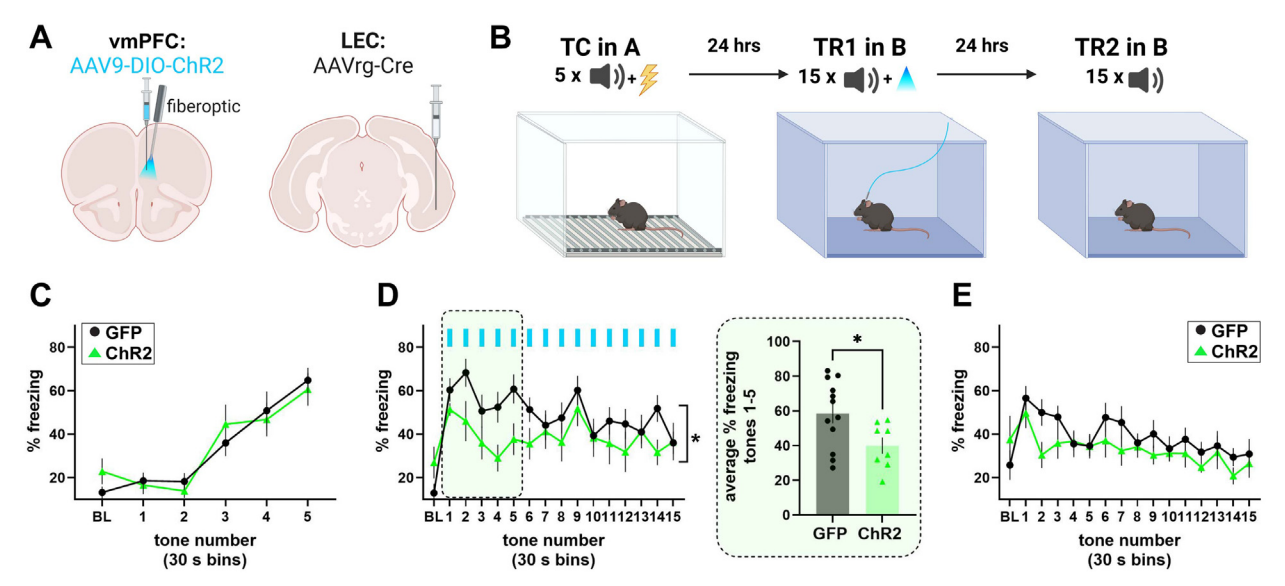


Figure 2. vmPFC-LEC cell activation in a different context than conditioning decreases threat expression. (A) Schematic of viral injections and fiberoptic placement. (B) Schematic for A-B-B TC, TR1, and TR2 paradigm. (C) Percent freezing during 30-second bins of baseline and tone presentation during TC in context A in GFP (black, n = 12) and ChR2 (green, n = 8) animals. (D) Percent freezing during 30-second bins of baseline and tone presentation during TR1 in context B. Thirty-second 20-Hz ChR2 pulses were delivered at the onset of each 30-second tone. Shaded box compares average percent freezing during the first 5 tones between GFP- and ChR2-injected animals. (E) Percent freezing during 30-second bins of baseline and tone presentation during TR2 in context B. $^*p < .05$. ChR2, channelrhodopsin-2; GFP, green fluorescent protein; LEC, lateral entorhinal cortex; TC, threat conditioning; TR1, first threat retrieval; TR2, second TR; vmPFC, ventromedial prefrontal cortex.

flexibly shape threat responding depending on the context in line with our hypothesis that vmPFC-LEC cells increase behavioral sensitivity rather than solely increase general threat responding.

vmPFC-LEC Cells Bidirectionally Regulate Context Threat Encoding and Expression

We next wanted to establish whether vmPFC-LEC cells can influence behavioral sensitivity to context in the absence of a tone cue using contextual TC. In mice expressing ChR2 in vmPFC-LEC cells (n=12 GFP, 8 ChR2), activation during contextual TC increased freezing levels compared with GFP control mice (Figure 3B) (two-way repeated-measures ANOVA across 8 1-minute epochs, main effect of virus condition: p=.050). The same mice showed increased freezing during the first 5 minutes of TR the following day compared with control mice (Figure 3C, D) (two-way repeated-measures ANOVA across 5 1-minute epochs, main effect of virus condition: p=.029).

In contrast, suppression of vmPFC-LEC cell activity with Halo in a separate cohort of mice during contextual TC did not immediately affect freezing levels (Figure 3F) (two-way repeated-measures ANOVA across 8 1-minute epochs, main effect of virus condition: p = .175). However, these mice that

received Halo stimulation during threat encoding showed decreased initial freezing during the first minute of TR the following day compared with GFP control mice (Figure 3G, H) (unpaired two-tailed t test, p = .036). Thus, using bidirectional optogenetic manipulations during threat encoding, we were able to demonstrate a causal role for vmPFC-LEC cells in contextual memory encoding that affects the ability to modulate behavioral sensitivity to contexts previously associated with threats.

vmPFC-LEC Projections Provide Excitatory Input Onto Layer 2/3 and Layer 5 LEC Cells

We next wanted to understand how vmPFC-LEC cells might influence contextual processing and the gain of behavioral output by the nature of their connectivity and cell-type identity. Using Rabies viral tracing, we identified direct inputs to vmPFC-LEC cells (Figure 4A–C; see Figure S4 for detailed cell counts for each mouse and control injections for viral "leakiness"). We observed that vmPFC-LEC cells are densely connected with prefrontal regions, namely the PL and orbitofrontal regions (Figure 4D, E), as well as sparse but substantial inputs from the anterior insula, BLA (Figure 4G), and claustrum (Figure 4F). Interestingly, vmPFC-LEC cells do not receive direct input from hippocampal regions; it may be that they

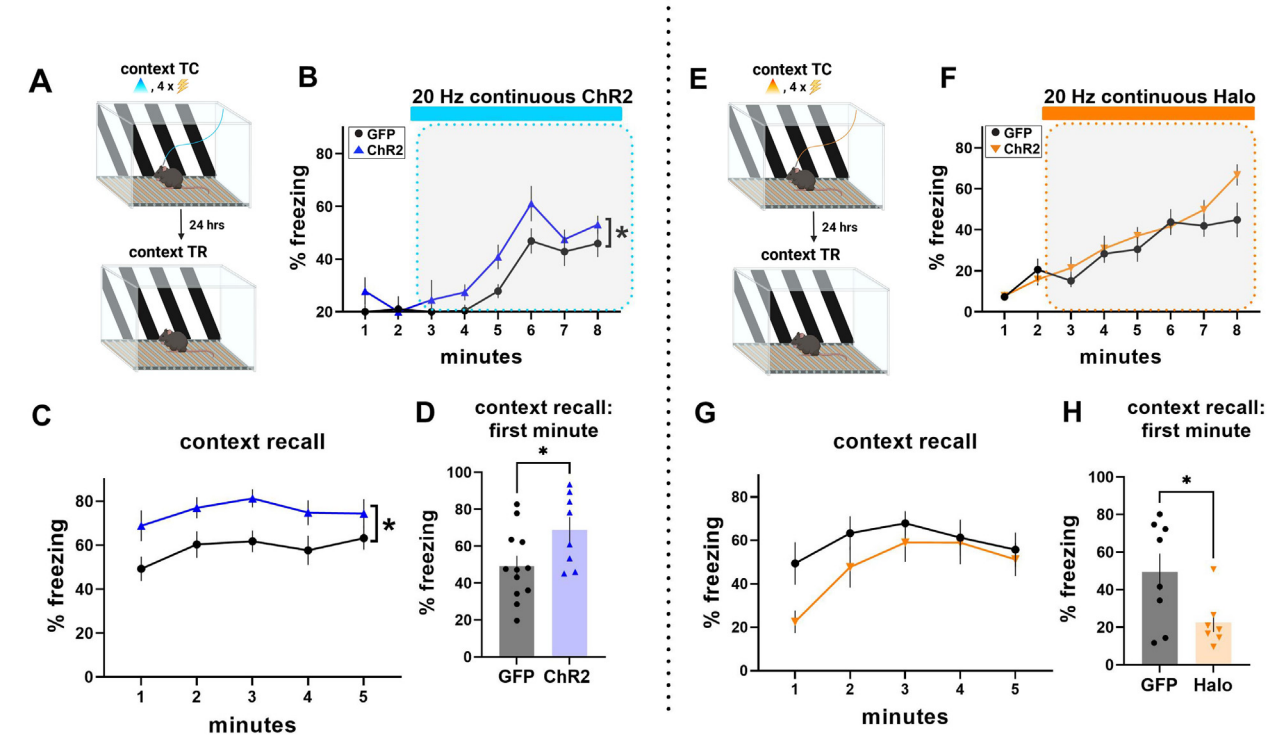


Figure 3. vmPFC-LEC cells bidirectionally modulate context recall. (A) Schematic of contextual TC (context TC) and retrieval (context TR) paradigm with ChR2 stimulation in context C. (B) Percent freezing during contextual TC in GFP (black, n = 12) and ChR2 (blue, n = 8) animals. Continuous 20-Hz laser stimulation was applied from minutes 2 to 8 of conditioning. (C) Percent freezing during context recall. (D) Percent freezing during the first minute of context recall. (E) Schematic of contextual TC paradigm with Halo stimulation. (F) Percent freezing during contextual TC in GFP (black, n = 8) and Halo (orange, n = 7) animals. Continuous 20-Hz laser stimulation was applied from minutes 2 to 8 of conditioning. (G) Percent freezing during context recall. (H) Percent freezing during the first minute of context recall. *p < .05. ChR2, channelrhodopsin-2; GFP, green fluorescent protein; Halo, halorhodopsin; LEC, lateral entorhinal cortex; TC, threat conditioning; TR, threat retrieval; vmPFC, ventromedial prefrontal cortex.

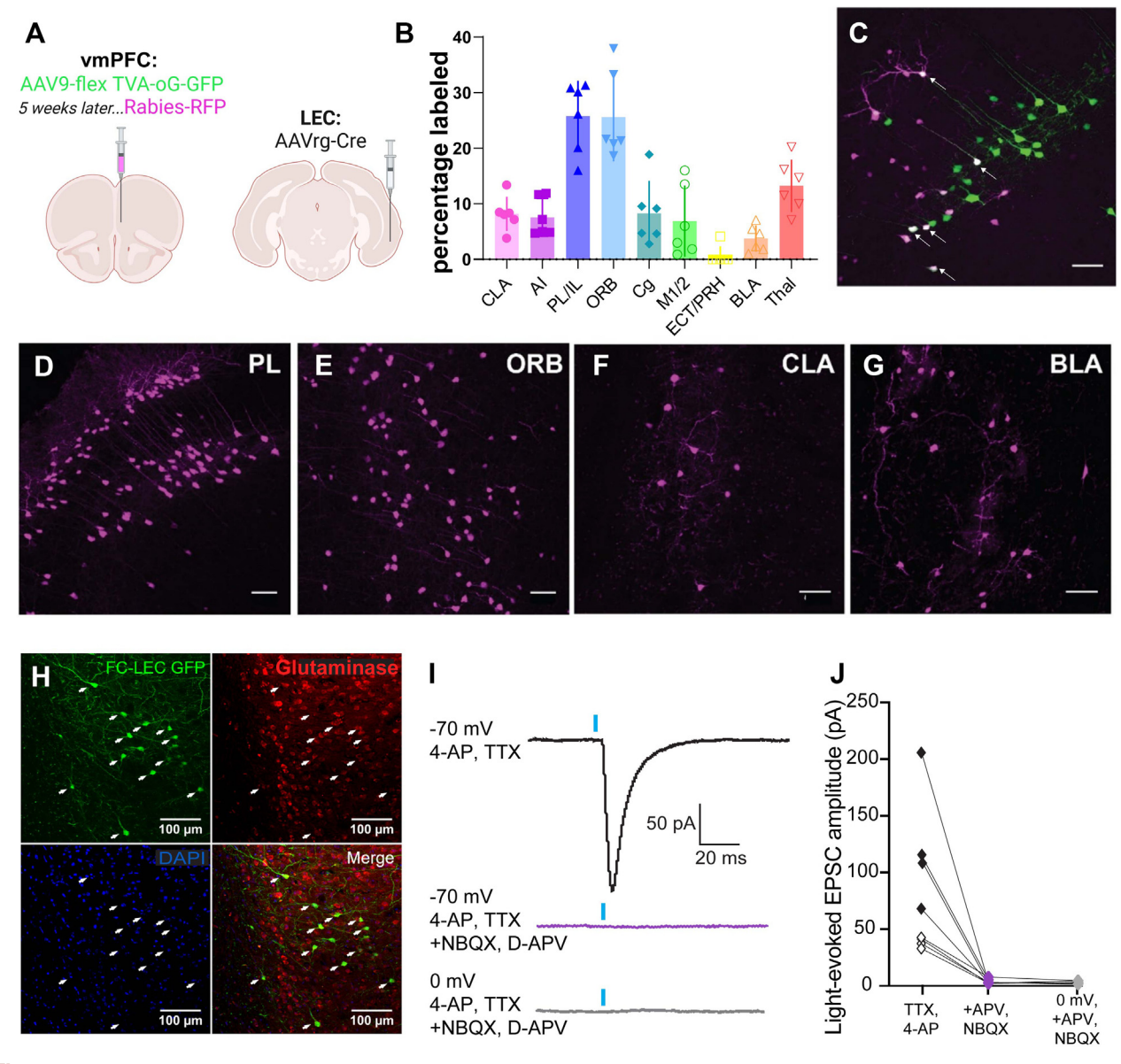
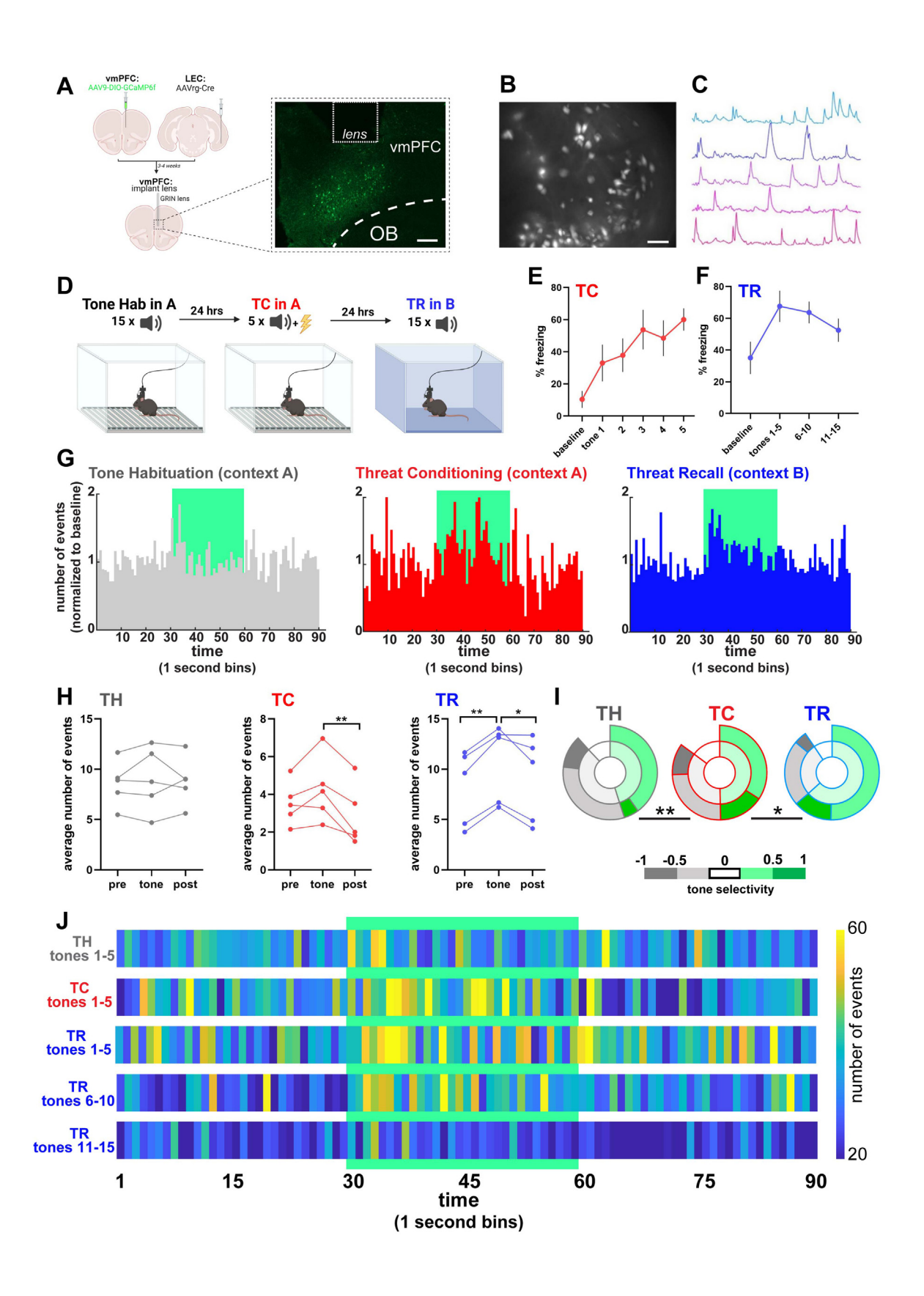


Figure 4. vmPFC-LEC cells receive dense cortical inputs and more sparse subcortical inputs and send glutamatergic projections to L2/3 and L5 in the LEC. (A) Schematic of viral injection. (B) Percentage of inputs received by vmPFC-LEC from the CLA, AI, PL/IL, ORB, Cg, M1/2, BLA, and thalamic regions in 6 mice. (C) Starter cells (white with white arrows) in IL among TVA-oG cells (green) and Rabies-labeled cells (magenta). Monosynaptic inputs from Rabies-labeled cells (magenta) in (D) PL, (E) ORB, (F) CLA, and (G) BLA. Scale bars = 50 μm. (H) Glutaminase staining (red) in GFP+vmPFC-LEC cells. (I) ChR2 light-evoked EPSCs (at −70 MV, black: baseline with TTX and 4-AP; purple: with TTX and 4-AP plus glutamatergic blockers NBQX and APV; at 0 MV, gray: with TTX and 4-AP plus glutamatergic blockers). (J) Summary plot of light-evoked EPSC amplitude during ChR2 stimulation with and without glutamate blockers from cells in L2/3 and L5. White diamonds, L5; black diamonds, L2/3. AI, anterior insula; BLA, basolateral amygdala; Cg, cingulate cortex; ChR2, channelrhodopsin-2; CLA, claustrum; ECT, ectorhinal cortex; EPSC, excitatory postsynaptic current; GFP, green fluorescent protein; IL, infralimbic cortex; L, layer; LEC, lateral entorhinal cortex; M1/2, motor cortices; ORB, orbitofrontal cortex; PI, prelimbic cortex; PRH, perirhinal cortex; Thal, thalamic regions; TTX, tetrodotoxin; vmPFC, ventromedial prefrontal cortex.

receive incoming contextual information from nearby PL cells, which receive contextual input from the ventral hippocampus.

We then used histological and electrophysiological methods to determine the cell-type identity of vmPFC-LEC cells. We found that vmPFC-LEC cells were predominately immunopositive for glutaminase, a glutamatergic cell marker (Figure 4H). We then used our previous intersectional viral strategy to

specifically drive channelrhodopsin expression in vmPFC-LEC cells to determine the sign of the input vmPFC-LEC cells provide and to which layers of the LEC. Stimulation of vmPFC-LEC cell terminals in both L2/3 and L5 of the LEC with channelrhodopsin resulted in a fast inward current in the presence of tetrodotoxin and 4-AP that was abolished with the glutamate receptor antagonists APV and NBQX (Figure 4I, J).



Calcium Imaging to Determine vmPFC-LEC Response Patterns to Cued TC and TR

Finally, we wanted to understand the endogenous activity of vmPFC-LEC cells during both TC and TR. We selectively expressed GCaMP6f in vmPFC-LEC cells using the previously described intersectional strategy (Figure 5A) and implanted a gradient-index lens over the vmPFC (Figure 5B). Four weeks after lens implantation, we collected calcium traces from vmPFC-LEC cells (Figure 5C) over 3 consecutive days during tone habituation (TH), TC, and TR (Figure 5D-F).

Exploratory calcium imaging in awake behaving mice revealed that vmPFC-LEC cells show increased activity during the 30-second tone presentations compared with 30-second pre- and post-tone intervals during the TR session, both cumulatively (Figure 5G, Kolmogorov-Smirnov test for difference in distributions of activity 30 seconds before vs. during tone: in TH, p=.586; in TC, p=.035; in TR, p<.001) and across mice (Figure 5H) (TR: one-way ANOVA, p=.003, honestly significant difference [Tukey] test: for pretone vs. tone, p<.01, for tone vs. post tone, p<.05) (Figure S5A–C) that was not present during TH.

vmPFC-LEC cells also showed a significant decrease in activity in the post-tone interval in both conditioning and retrieval sessions but not TH (TC: one-way ANOVA, p = .007, honestly significant difference [Tukey] test for tone vs. posttone, p < .01; TR: one-way ANOVA, p = .003, honestly significant difference [Tukey] test for tone vs. post-tone, p < .05). The largest increase in activity was found within 10 seconds of tone onset during the first 5 tones of TC and TR, though toneonset-related increases in activity persisted to a lesser extent throughout retrieval (Figure 5J). The selectivity of vmPFC-LEC cells for tone significantly increased from TH to TC to TR, with more than 60% of cells showing selectivity for tone over the pretone interval during retrieval (Figure 5I) (unpaired two-tailed t test: selectivity for tone in TH vs. TC, p = .008; in TC vs. TR, p = .039). The increase in cumulative activity to, as well as selectivity for, the tone cue in TC and TR suggests a shaping of vmPFC-LEC responsiveness to tone that is increased as threat memory is formed and subsequently retrieved.

We then tracked the same cells across TC and TR (n=257 cells of a total 363 cells imaged) and found that roughly 25% of vmPFC-LEC cells (79 of 257 cells) (purple in Figure 6A, B, D) are selective for tone in both conditioning and retrieval, independent of the context in which tone is presented. In contrast, roughly half of cells selective for the tone in one condition either no longer respond to, reverse, or lose their selectivity to the tone in the other condition (70 of 149 cells selective for

tone in TC [Figure 6A, E], 108 of 187 cells selective for tone in TR [Figure 6B, F]). Additionally, another independent subset of cells was only active in either context A or context B (Figure 6C), further suggesting a sensitivity of vmPFC-LEC cells to context. We also examined how freezing levels correlated with vmPFC-LEC activity and found that the correlation between freezing and activity increases from TC to TR both across average freezing levels and across correlation coefficients from each individual cell (Figure S6A-D).

To summarize, as a population, vmPFC-LEC cells show an increase in responsiveness and selectivity to tone that increases from TH to TC and peaks during threat expression (initial tones during TR). Interestingly, when individual cells are tracked across conditioning (context A) and retrieval (context B), subpopulations of vmPFC-LEC cells seem to either encode tone in a context-invariant or context-dependent manner.

DISCUSSION

Here, we show that vmPFC-LEC cells can bidirectionally modulate context encoding of threat, shaping behavioral responding during TR. In both cued threat expression and contextual recall, vmPFC-LEC cells seem to modulate the gain of behavioral output in response to incoming contextual information to shift behavior in a more adaptive direction (Supplemental Discussion). Our examination of the inputs and outputs of vmPFC-LEC cells using Rabies tracing and channelrhodopsin-assisted electrophysiology further reveals large inputs from the mPFC, anterior insula, claustrum, and BLA as well as a monosynaptic glutamatergic output onto layers 2/3 and 5 of the LEC. The glutamatergic nature of this projection was surprising given that behavioral gain control is traditionally thought to rely on GABAergic (gamma-aminobutyric acidergic) circuits (Supplemental Discussion). Finally, we demonstrate that vmPFC-LEC cells are responsive to threat-associated cues in a context-dependent manner and that this responsivity may underlie their ability to flexibly shape behavior in response to threat-associated cues in a contextspecific manner.

vmPFC-LEC Cells and Previous Data on IL in Threat Processing

IL, a critical subregion of the vmPFC, has previously been shown to play a role in extinction learning as well as decreasing threat and anxiety-like behavior more generally (3,5,6,28–31). However, other studies demonstrate a critical role for IL in extinction memory recall (32,33). A recent review by Gonzalez and Fanselow (34) suggested that in

Figure 5. vmPFC-LEC cells show increased activity and selectivity for tone during TC and threat expression. **(A)** Schematic of viral injections and GRIN lens placement. Inset, representative image of lens placement and GCaMP expression. Scale bar = 500 μm. **(B)** Maximum projection of vmPFC-LEC cells from representative animal. Scale bar = 50 μm. **(C)** Delta F/F traces from 5 individual vmPFC-LEC cells. **(D)** Schematic for behavioral battery performed during imaging. **(E)** Percent freezing during baseline and tone presentation in TC in context A. **(F)** Percent freezing during baseline and tone presentation during TR in context B. **(G)** Normalized peristimulus time histogram across all cells during TH (n = 272 cells), TC (n = 313 cells), and TR (n = 298 cells), aligned to 30 seconds before tone. Normalized to average number of cumulative events in 30-second pretone interval. Tone indicated by green shading. **(H)** Average number of events in each mouse (n = 5 mice) during cumulative pretone, tone, and post-tone intervals for TH, TC, and TR. **(I)** Selectivity [(number of events during tone – number of events during 30 seconds before tone) / (number of events during tone + number of events during 30 seconds before tone)] for 30-second tone interval vs. 30-second pretone interval. Greater than zero indicates selective for tone (green), <0 indicates selective for pretone (gray), equal to zero indicates nonselective (white). **(J)** Heatmap of cumulative activity 30 seconds before, during, and after tone presentation during TH, (tones 1–5), TC, and TR, for all 363 cells imaged. One-second bins. Green box indicates tone. p < 0.05, threat conditioning; TH, tone habituation; TR, threat retrieval; vmPFC, ventromedial prefrontal cortex.

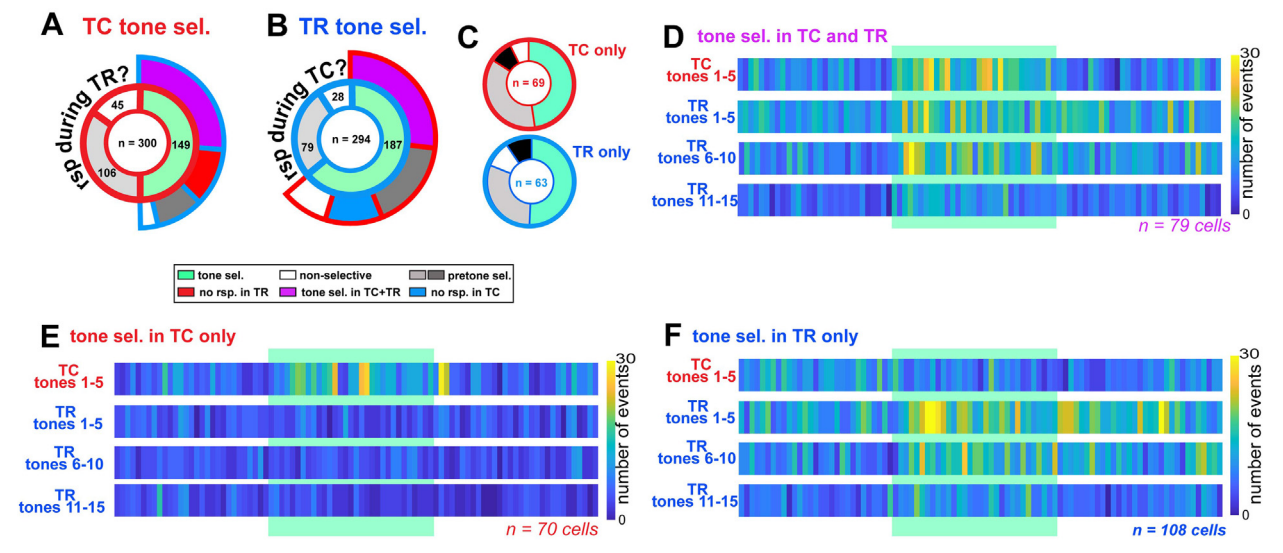


Figure 6. vmPFC-LEC subpopulations show different tone selectivity in threat-related and neutral contexts. (A) Selectivity map for cells selective for tone during TC (inner ring) and their selectivity for tone during TR (outer ring). (B) Selectivity map for cells selective for tone during TR (inner ring) and their selectivity for tone during TC (outer ring). (C) Selectivity map for cells only active in context A (top) or in context B (bottom). (D) Heatmap of cumulative activity during TC and TR tones from 30 seconds before the beginning to 30 seconds after the end of tone presentation in cells selective for tone in both TC and TR (purple section of selectivity plot in panels (A, B). Green box indicates tone. (E) As in panel (D) but for cells only selective for tone in TC (red section of selectivity plot in panel (A). (F) As in panel (D) but for cells only selective for tone in TR (blue section of selectivity plot in panel (B). rsp, response; sel., selection; TC, threat conditioning; TR, threat retrieval; vmPFC, ventromedial prefrontal cortex.

contrast to promoting extinction/threat inhibition, IL may instead shape contextual responsiveness, citing literature from both threat processing and reward seeking in which IL lesions or inactivation disrupt contextual processing rather than simply affecting the ability of the animal to inhibit threat responding.

Our results seem to lie somewhere between these 2 contrasting hypotheses (though note that we targeted the anteriormost portion of IL and posterior MO) (Figure S7). In contrast to the hypothesis that IL primarily promotes threat inhibition, we show that vmPFC-LEC activation during threat expression can push behavior in different directions depending on the context. These results differ from previous IL lesion and pharmacology studies that show no effects of IL lesions on threat expression as well as recent findings that MO activation impairs TR across contexts (35). While it is clear that vmPFC-LEC cells promote behavioral sensitivity in different contexts, our results also do not align with the description of IL as a region that promotes generality of behavior (34); activation of vmPFC-LEC cells improves within-session contextual discrimination, increasing freezing in a previously threatassociated context and decreasing freezing in a novel context with no threat associations, rather than driving freezing in a consistent direction across contexts. vmPFC-LEC cells may drive freezing in opposing directions depending on the context via their downstream inputs to the LEC, different subpopulations of which project to distinct hippocampal subregions (Supplemental Discussion). Future experiments distinguishing which LEC subpopulations vmPFC-LEC cells synapse onto will provide insight as to how these cells push behavior in different directions.

ACKNOWLEDGMENTS AND DISCLOSURES

This work is supported by the National Institutes of Health (NIH) (Grant Nos. T32-MH125786 and TL1-TR002555 [to EH], Grant Nos. P50-MH115874 and R01-MH108665 [to KJR], and Grant No. R01-MH111684 [to SHS]), the Jonathan Edward Brooking Mental Health Research Award (to EH), the Eric Dorris Memorial Research Award (to EH), and the McLean Frazier Fund (to KJR).

EH, SHS, and KJR designed all experiments. EH and KJR wrote the manuscript. EH performed all viral injections, implantations, imaging, optogenetic behavioral experiments, and histology. AP performed in vivo whole-cell electrophysiology. YG performed glutaminase immunohistochemistry. KH performed control Rabies injections.

We acknowledge David Schneider for careful reading of the manuscript and members of the Ressler lab at McLean for their support, and the animal care staff at McLean Hospital.

All schematics and illustrations were created with BioRender.com.

KJR has performed scientific consultation for Bioxcel, Bionomics, Acer, Takeda, and Jazz Pharma; serves on Scientific Advisory Boards for Sage and the Brain Research Foundation; has received sponsored research support from Takeda, Brainsway, and Alto Neuroscience; and receives research funding from the NIH. All other authors report no biomedical financial interests or potential conflicts of interest.

ARTICLE INFORMATION

From the Department of Cell Biology, Duke University School of Medicine, Durham, North Carolina (EH, AP, YG, KH, SHS); and Department of Psychiatry, McLean Hospital, Harvard Medical School, Belmont, Massachusetts (EH, KJR).

Address correspondence to Kerry J. Ressler, M.D., Ph.D., at kressler@mclean.harvard.edu.

Received Aug 30, 2022; revised and accepted Jan 11, 2023.

Supplementary material cited in this article is available online at https://doi.org/10.1016/j.biopsych.2023.01.009.

REFERENCES

- 1. Bowers ME, Ressler KJ (2015): An overview of translationally informed treatments for posttraumatic stress disorder: Animal models of Pavlovian fear conditioning to human clinical trials. Biol Psychiatry 78:F15-F27
- 2. Fenster RJ, Lebois LAM, Ressler KJ, Suh J (2018): Brain circuit dysfunction in post-traumatic stress disorder: From mouse to man. Nat Rev Neurosci 19:535-551.
- Vidal-Gonzalez I, Vidal-Gonzalez B, Rauch SL, Quirk GJ (2006): Microstimulation reveals opposing influences of prelimbic and infralimbic cortex on the expression of conditioned fear. Learn Mem 13:728-733.
- 4. Sierra-Mercado D, Corcoran KA, Lebrón-Milad K, Quirk GJ (2006): Inactivation of the ventromedial prefrontal cortex reduces expression of conditioned fear and impairs subsequent recall of extinction. Eur J Neurosci 24:1751-1758.
- 5. Do-Monte FH, Manzano-Nieves G, Quiñones-Laracuente K, Ramos-Medina L, Quirk GJ (2015): Revisiting the role of infralimbic cortex in fear extinction with optogenetics. J Neurosci 35:3607-3615.
- 6. Burgos-Robles A, Vidal-Gonzalez I, Santini E, Quirk GJ (2007): Consolidation of fear extinction requires NMDA receptordependent bursting in the ventromedial prefrontal cortex. Neuron 53:871-880
- 7. Pennington ZT, Anderson AS, Fanselow MS (2017): The ventromedial prefrontal cortex in a model of traumatic stress: Fear inhibition or contextual processing? Learn Mem 24:400-406.
- 8. Zelikowsky M, Hersman S, Chawla MK, Barnes CA, Fanselow MS (2014): Neuronal ensembles in amygdala, hippocampus, and prefrontal cortex track differential components of contextual fear. J Neurosci 34:8462-8466.
- 9. Zelikowsky M, Bissiere S, Hast TA, Bennett RZ, Abdipranoto A, Vissel B, Fanselow MS (2013): Prefrontal microcircuit underlies contextual learning after hippocampal loss. Proc Natl Acad Sci USA
- 10. Maren S, Phan KL, Liberzon I (2013): The contextual brain: Implications for fear conditioning, extinction and psychopathology. Nat Rev Neurosci 14:417-428.
- 11. Josselyn SA, Tonegawa S (2020): Memory engrams: Recalling the past and imagining the future. Science 367:eaaw4325.
- 12. Guthman EM, Garcia JD, Ma M, Chu P, Baca SM, Smith KR, et al. (2020): Cell-type-specific control of basolateral amygdala neuronal circuits via entorhinal cortex-driven feedforward inhibition. eLife 9: e50601.
- 13. Vandrev B. Garden DLF. Ambrozova V. McClure C. Nolan MF. Ainge JA (2020): Fan cells in Layer 2 of the lateral entorhinal cortex are critical for episodic-like memory. Curr Biol 30:169-175.e5.
- 14. Wilson DIG, Langston RF, Schlesiger MI, Wagner M, Watanabe S, Ainge JA (2013): Lateral entorhinal cortex is critical for novel objectcontext recognition. Hippocampus 23:352-366.
- 15. Wilson DIG, Watanabe S, Milner H, Ainge JA (2013): Lateral entorhinal cortex is necessary for associative but not nonassociative recognition memory. Hippocampus 23:1280-1290.
- Morrissey MD, Takehara-Nishiuchi K (2014): Diversity of mnemonic function within the entorhinal cortex: A meta-analysis of rodent behavioral studies. Neurobiol Learn Mem 115:95-107.
- 17. Fernández-Ruiz A, Oliva A, Soula M, Rocha-Almeida F, Nagy GA, Martin-Vazquez G, Buzsáki G (2021): Gamma rhythm communication between entorhinal cortex and dentate gyrus neuronal assemblies. Science 372:eabf3119.

Montchal ME, Reagh ZM, Yassa MA (2019): Precise temporal memories are supported by the lateral entorhinal cortex in humans. Nat Neurosci 22:284-288.

vmPFC-LEC Circuit in Threat Response

- Khan UA, Liu L, Provenzano FA, Berman DE, Profaci CP, Sloan R, et al. (2014): Molecular drivers and cortical spread of lateral entorhinal cortex dysfunction in preclinical Alzheimer's disease. Nat Neurosci 17:304-311.
- Maass A, Lockhart SN, Harrison TM, Bell RK, Mellinger T, Swinnerton K, et al. (2018): Entorhinal tau pathology, episodic memory decline, and neurodegeneration in aging. J Neurosci 38:530-543.
- Maren S, Fanselow MS (1997): Electrolytic lesions of the Fimbria/ fornix, dorsal hippocampus, or entorhinal cortex produce anterograde deficits in contextual fear conditioning in rats. Neurobiol Learn Mem 67:142-149
- Phillips RG, LeDoux JE (1995): Lesions of the fornix but not the entorhinal or perirhinal cortex interfere with contextual fear conditioning. J Neurosci 15:5308-5315.
- Majchrzak M, Ferry B, Marchand AR, Herbeaux K, Seillier A, Barbelivien A (2006): Entorhinal cortex lesions disrupt fear conditioning to background context but spare fear conditioning to a tone in the rat. Hippocampus 16:114-124.
- Ji J, Maren S (2008): Lesions of the entorhinal cortex or fornix disrupt the context-dependence of fear extinction in rats. Behav Brain Res 194:201-206.
- East BS, Brady LR, Quinn JJ (2021): Differential effects of lateral and medial entorhinal cortex lesions on trace, delay and contextual fear memories. Brain Sci 12:34.
- Gao Y, Hisey E, Bradshaw TWA, Erata E, Brown WE, Courtland JL, et al. (2019): Plug-and-play protein modification using homologyindependent universal genome engineering. Neuron 103:583-597.e8.
- Purkey AM, Woolfrey KM, Crosby KC, Stich DG, Chick WS, Aoto J, Dell'Acqua ML (2018): AKAP150 palmitoylation regulates synaptic incorporation of Ca2+-permeable AMPA receptors to control LTP. Cell Rep 25:974-987.e4.
- Sotres-Bayon F, Quirk GJ (2010): Prefrontal control of fear: More than just extinction. Curr Opin Neurobiol 20:231-235.
- Shimizu T, Minami C, Mitani A (2018): Effect of electrical stimulation of the infralimbic and prelimbic cortices on anxiolytic-like behavior of rats during the elevated plus-maze test, with particular reference to multiunit recording of the behavior-associated neural activity. Behav Brain Res 353:168-175.
- Liu WZ, Zhang WH, Zheng ZH, Zou JX, Liu XX, Huang SH, et al. (2020): Identification of a prefrontal cortex-to-amygdala pathway for chronic stress-induced anxiety. Nat Commun 11:2221.
- Bloodgood DW, Sugam JA, Holmes A, Kash TL (2018): Fear extinction requires infralimbic cortex projections to the basolateral amygdala. Transl Psychiatry 8:60.
- Kim HS, Cho HY, Augustine GJ, Han JH (2016): Selective control of fear expression by optogenetic manipulation of infralimbic cortex after extinction. Neuropsychopharmacology 41:1261-1273.
- Marek R, Jin J, Goode TD, Giustino TF, Wang Q, Acca GM, et al. (2018): Hippocampus-driven feed-forward inhibition of the prefrontal cortex mediates relapse of extinguished fear. Nat Neurosci 21:384-392.
- Gonzalez ST, Fanselow MS (2020): The role of the ventromedial prefrontal cortex and context in regulating fear learning and extinction. Psychol Neurosci 13:459-472.
- Sun CF, Chang CH (2022): Aberrant orbitofrontal cortical activation interferes with encoding of Pavlovian fear conditioning. Front Behav Neurosci 16:981041.